Heuchel, M.; Razzaq, M.Y.; Kratz, K.; Behl, M.; Lendlein, A.:

Modeling the heat transfer in magneto-sensitive shape-memory polymer nanocomposites with dynamically changing surface area to volume ratios

In: Polymer (2015) Elsevier

DOI: 10.1016/j.polymer.2015.03.063

Modeling the heat transfer in magneto-sensitive shape-memory polymer nanocomposites with dynamically changing surface area to volume ratios

M. Heuchel, M.Y. Razzaq, K. Kratz, M. Behl, A. Lendlein*
Institute of Biomaterial Science and Berlin-Brandenburg Center for Regenerative Therapies Helmholtz-Zentrum Geesthacht, Kantstr. 55, 14513 Teltow, Germany
*Corresponding author: andreas.lendlein@hzg.de, Tel.: +49 (0)3328 352 450; fax: +49 (0)3328 352 452

Abstract:
Magneto-sensitive shape-memory polymer nanocomposites (SMPNCs) enable non-contact actuation of a shape-memory effect (SME) by inductive heating in an alternating magnetic field (AMF). Hereby, the achievable temperature (T_{max}) at fixed magnetic field strength and frequency is depending on the amount and type of incorporated magnetic fillers as well as on surface area to volume (S/V) ratio of the test specimen.
Here we present a heat transfer model for predicting T_{max} of SMPNCs samples with different S/V ratios when exposed to an AMF. The obtained temperature difference between sample and surrounding in an AMF of constant magnetic field strength decreases at uni-axial deformation with the square root of the stretching ratio. The model was validated with magnetically heating experiments of two different SMPNC systems (comprising crystallizable or amorphous switching segments) containing the same magnetic nanoparticles, while the magnetic field strength (H) was varied from 7 to 27 $kA \cdot m^{-1}$ at a fixed frequency of 258 kHz. The experimentally achieved temperatures at deformations up to 50% could be predicted with an accuracy below 6%. Finally the model was applied in a principle design study of a device consisting of a rolled SMPNC stripe, which was stepwise opened by increasing H. The modeling approach might be helpful to predict the temperature profiles of SMPNCs which were heated by other mechanisms, e.g., radiofrequency or near IR.

Keywords:
modeling; nanocomposites; shape-memory polymers

1. Introduction

Shape-memory polymers (SMPs) and composites thereof are able to change their shape in a predefined way from a temporary programmed to their original shape when exposed to a suitable stimulus such as heat and when a specific response temperature is exceeded [1-8]. The response temperature is typically related to a thermal transition (T_{trans}) of the SMPs´ switching domains, which can either be a melting temperature (T_m) or a glass transition temperature (T_g). Thermal activation is typically achieved through the transfer of thermal energy from the environment directly to the programmed SMP via conduction, convection or thermal radiation. The kinetics of the observed T-increase depends on the heat capacity of the system and possible thermal phase transitions as in case of semi-crystalline materials. An alternative non-contact way of heating is inductive heating of magneto-sensitive shape-memory polymer nanocomposites (SMPNCs) containing magnetic nanoparticles (MNPs) embedded in the SMP matrix [9-20]. These particles heat the SMP material via hysteresis loss and/or superparamagnetism related processes when the composite is exposed to an alternating magnetic field (AMF). Besides the generation of heat inside the composite sample caused by inductive heating of the magnetic fillers, the heat dissipation (heat loss) at the surface, which is in contact to the surrounding environment, has to be considered in a steady state. In this context the surface area to volume (S/V) ratio of the test specimen is an important parameter [14, 17, 20]. The higher the S/V ratio, the lower is the maximum temperature (T_{max}) of the nanocomposite. To ensure an accurate control of T_{max} as well as to minimize changes in S/V ratios during shape changes, the majority of shape-memory experiments in AMF have been conducted using bending experiments [13, 14, 17].

The main objective of this paper is to derive a model equation for the obtainable T_{max}-values during inductive heating under dynamic deformation of the sample in the AMF. To obtain such a relation, we have (i) to consider the production of heat in the sample, then (ii) to find a relation for the heat transport in the sample, and (iii) to derive a relation for the achieved temperature of the sample in the quasi-equilibrium state. The next objective of this paper is the detailed validation of the model by experimental data. For our investigations we selected SMPNCs composed of one type of MNPs, which were embedded in two different SMP polymer matrices, while the MNP content was varied. Our third objective is an application of the theoretical considerations to design a specific SMPNC device, which is controlled by means of the S/V ratios.

1.1 Applied shape-memory polymer nanocomposites (SMPNCs)

In the later validation experiments (section 4) SMPNCs with two different polymer matrices were used: (i) a thermoplastic polyetherurethane (PEU) containing amorphous switching domains [15, 18, 21, 22] and (ii) a chemically crosslinked polymer network based on poly(*ε*-caprolactone) (cPCL) with crystallizable switching domains [17, 18, 23]. PEU exhibits a mixed glass transition of $T_{g,mix}$ = 74-76 °C and was synthesized from methylene bis(*p*cyclohexyl isocyanate) (H_{12}MDI), 1,4-butanediol (1,4-BD), and poly(tetramethylene glycol) (PTMG) [22, 24]. The crosslinked cPCL composites (cPCLC) were synthesized by thermally-initiated crosslinking of crystallizable poly(*ε*-caprolactone)diisocyanatoethyl dimethacrylate (PCLDIMA) (T_m = 51-52 °C) with an average molecular weight of M_n ~ 8300 $g \cdot mol^{-1}$ in the presence of MNP [17, 25]. All investigated SMPNCs contained the same type of silica coated magnetite nanoparticles (AdNano MagSilica 50, Degussa, Hanau, Germany) with a mean aggregate size of 90 nm, a mean domain size of 20–26 nm, and a magnetic domain content of 50–60 wt% [15, 26]. The Magsilica nanoparticles are assumed as (super)-paramagnetic [27].

For validation experiments, both types of SMPNCs (amorphous PEUC and crystallizable cPCLC) were applied with a MNP content of 5, 10, and 15 wt%. The investigated samples are named PEUC05, PEUC10, PEUC15, cPCLC05, cPCLC10, and cPCLC15. Detailed data for the nanocomposites of both polymer types were already published for PEUC [18] and cPCL [25], except for cPCL15 which are presented here for the first time. Values characterizing the thermal properties of the investigated SMPNCs are provided in Table S1 as supplementary data (see Appendix). The distribution of the MNPs within the SMPNCs was tested by microscopic analysis and had shown individual, small clusters in the submicrometer length-scale [18, 25]. The transition temperatures (T_{trans}) of the SMPNCs were determined by differential scanning calorimetry (DSC) and indicated a strong melting peak for cPCLCxx at 52 °C which was not affected by the incorporation of MNP (see Table S1). The chemical structure of PEU consists of H_{12}MDI/1,4-BD hard segments and H_{12}MDI/PTMEG soft segments, in which the content of H_{12}MDI/1,4-BD was 58 wt% according to the calculation from ^1H-NMR spectroscopy [18]. DSC thermograms of the PEUC revealed a pronounced glass transition temperature T_g at 55 °C attributed to the mixed phase of hard and soft segments ($T_{g,mix}$). In the *tan δ* curve obtained in DMTA measurements two additional peaks were observed for the plain PEU and its composites**,** corresponding to the T_g of the soft domains (-40 °C) and of the hard domains (140 °C). A broad peak with the maximum at

around 74 °C reflects the $T_{g,mix}$, which was only slightly changed when MNP were added (see Supplementary information, Table S1).

The main objective of this paper is the mentioned model equation for the obtainable T_{max}-values of an SMPNC sample during inductive heating under dynamic deformation of this sample in the AMF. After explanation of the applied experimental methods for the later model validation, it follows the description of the model with derivation of the basic equation. Then, the developed model is validated, first with experiments showing the behavior of cPCLC and PEUC composite samples comprising different MNP content with constant S/V ratio in an AMF at different field strengths H, second with magnetic heating experiments, where the S/V ratio of the samples was varied by uniaxial deformation, and third with a design example for a device, where the recovery process of a magneto-sensitive SMPNC, i.e. the stepwise uncoiling of a rolled stripe, by stepwise increase of the field strength H was investigated. The paper closes with general conclusions.

2. Experimental

2.1 Magnetic heating experiments

Inductive heating was accomplished by positioning the SMPNC sample in an alternating magnetic field. The device consisted of a high-frequency (HF) generator (TIG 5/300; Huettinger Electronic, Freiburg, Germany) and a water-cooled copper coil (6 loops, diameter 40 mm, height 45 mm) as described previously [15, 18]. The magnetic field strength H was increased stepwise (≈ 1 kA·m^{-1} per step) from H_0 = 0 kA·m^{-1} to H_{max} = 29 kA·m^{-1} at ambient temperature and constant frequency of f = 258 kHz. After each step a waiting period of 3 minutes was used for equilibration. An IR pyrometer (Metis MY84, Sensortherm; Frankfurt) was used for non-contact measuring of the sample temperature T_{max}.

2.2 Uniaxial stress strain experiments in a magnetic field

The magneto-mechanical experiments were carried out with a Zwick Z2.5 (Zwick, Ulm, Germany) tensile tester, which was combined with the HF generator according to a method recently described in [18]. The SMPNC samples were fixed with plastic clamps in the center of the inductor. Experiments were performed at ambient temperature. After T_{max} was reached at the selected magnetic field strength H, a stepwise deformation of the sample (10% increments) was carried out with a strain rate of 5 mm·min^{-1} to a final elongation of 50%.

After each elongation step, the sample was allowed to achieve equilibrium for five minutes. During the uniaxial deformation T_{max} was measured with the IR pyrometer.

2.3 Shape-change experiments in a stepwise increased magnetic field

A cPCLC10 stripe (50 mm x 4 mm x 1 mm) was rolled at a temperature of 70 °C to a spiral. Then the sample was cooled down again to room temperature. Before, the strip was covered with a thermally conductive silicon paste to ensure better heat transfer to reach a quick thermal equilibrium. The spiral sample was placed in the device of the magnetic heating experiments (see section 2.1). The magnetic field strength H was increased stepwise (≈1 $kA \cdot m^{-1}$ per step) from H_0 = 0 $kA \cdot m^{-1}$ to H_{max} = 20.7 $kA \cdot m^{-1}$ at ambient temperature and a constant frequency of f = 258 kHz. At each step, after a waiting period of 3 minutes, the sample was photographed, and the outer diameter of the sample was measured.

3. Model development

3.1 Heat generation in an alternating magnetic field

Heat generation from MNP exposed to an AMF occurs primarily by relaxation losses and hysteresis losses. The dominant mechanism is determined by particle size and AMF parameters (magnetic field strength *H*, frequency *f*). Superparamagnetic MNPs can exhibit hysteresis loops in an AMF depending on the frequency, however the primary loss mechanisms are relaxational. A model for heat generation from superparamagnetic MNP has been previously proposed by Rosensweig [28]. After this model, the magnetically induced volumetric power dissipation can be expressed as

$$P_M = \pi \mu_0 \chi_0 H^2 f \frac{2\pi f \tau}{1+(2\pi f \tau)^2} \quad (1)$$

where μ_0 is the permeability of free space, χ_0 is the equilibrium susceptibility, and τ is the effective relaxation time. The effective relaxation time is determined by two relaxation processes. When an external field, applied to a MNP, is reduced to zero, its magnetization decreases to zero due to ambient thermal energy; this relaxation can be Brownian or Néel and occurs rapidly as the AMF varies between positive and negative values of its maximum amplitude. In principle Brownian and Néel relaxation processes occur in parallel and determine the effective relaxation time τ. In Néel relaxation, the magnetic moment of the particle rotates internally to align with the field while in Brownian relaxation, the particle

physically rotates to align the moment with the field. The second process, a reorientation of the MNP itself, is excluded in nanocomposites, where the MNP is fixed in a polymer matrix. Eq. (1) shows that at constant high frequency the magnetically induced power loss P_M is proportional to H^2, i.e. it can be presented by a relation

$$P_M = R_H H^2 \tag{2}$$

where R_H is a magnetic field resistance constant summarizing the contribution from Néel relaxation and possible other loss mechanisms. We assume that this power loss in the magnetic particles is completely transferred into heat, i.e. it creates a heat flow $\dot{q}$. This heat flow can be described by Fourier's law, i.e. the time rate of the heat transfer through the polymer composite is proportional to the (negative) gradient in temperature ΔT, and to the surface area A of the sample. If α is the materials heat conductivity, it follows for a (as homogeneous assumed) sample of 1-D geometry between two endpoints at distance d at constant temperatures an equation for the heat flow rate (or heat emission) [29]:

$$\dot{q} = -\frac{\alpha A}{d}\Delta T \tag{3}$$

By equalization of the magnetically induced power $R_H H^2$ (2) and the heat emission (3) a quadratic relation follows for the temperature increase $\Delta T(H) = T_{\max}(H) - T_{RT}$ of the sample with respect to the applied magnetic field strength H, and for this temperature increase the following relation is obtained:

$$\Delta T(H) = T_{\max}(H) - T_{RT} = (dR_H / \alpha A)H^2 = kH^2 \tag{4}$$

where k is a constant, which depends on MNP type and content, geometry parameters of the sample including the surface area, frequency of the magnetic field, and thermal conductivity.

3.2 Relation for the temperature effect during stretching in a magnetic field H.

From Eq. (4) it follows that the temperature increase ΔT for a sample at constant magnetic field strength H is inversely proportional to the surface area A of the sample. For the temperature effect during stretching a relation between surface area A and deformation is necessary. Fig. 1 sketches the situation for a polymer stripe of initial length L_{x0}, and width L_{y0}.

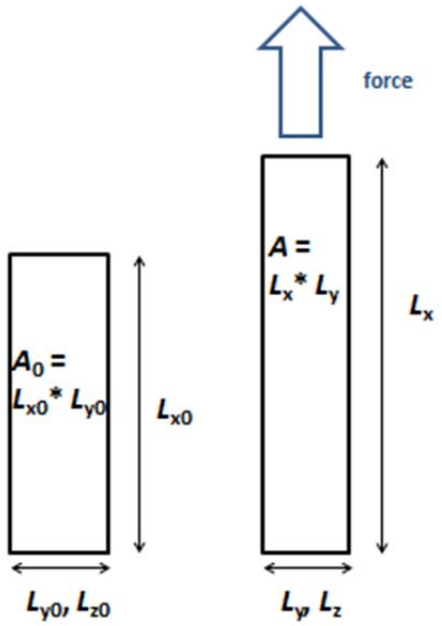

Fig. 1 Sketch for the uni-axial deformation of parallelepipeds in x-direction.

The volume of the sample stripe is $V_0 = L_{x0}L_{y0}L_{z0}$. Let's assume, the stripe is stretched in an uni-axial deformation from L_{x0} to the length L_x. The width will change (reduce) to L_y. The volume of the stripe after the deformation is then $V = L_x L_y L_z$. If the sample is incompressible, the volume remains constant during this deformation, i.e. $V = V_0$. Using the stretch ratio or extension ratio $\lambda_i = L_i / L_{i0}$, $i = x, y, z$, the incompressibility of the sample can be expressed by the general relation between the three stretch ratios

$$\lambda_x \lambda_y \lambda_z = 1 \tag{5}$$

Assuming a square-shaped cross-section, i.e. $\lambda_y = \lambda_z$, it follows from Eq. (5) an equation that characterize the width of the stripe as function of its length, i.e. $\lambda_y = 1/\sqrt{\lambda_x}$. With this relation, we obtain for the surface area ratio between deformed and non-deformed stripe (see Fig. 1) the following relation

$$\frac{A}{A_0} = \frac{L_x L_y}{L_{x0} L_{y0}} = \lambda_x \lambda_y = \sqrt{\lambda_x} = \sqrt{1 + \varepsilon_x} \tag{6}$$

where the general definition of the engineering strain,

$$\varepsilon \equiv \frac{L - L_0}{L_0} = \frac{L}{L_0} - 1 \tag{7}$$

is used. It should be noted that the same relation between the ratio of surface areas and the engineering strain ε, as presented in Eq. (6), can be also derived for constant sample thickness $L_z = L_{z0}$, or for a cylindrical sample of initial length L_0 and radius r_0. The surface area of the sample is $A_0 = 2\pi r_0 L_0$, and the volume of the sample $V_0 = \pi r_0^2 L_0$ may be expressed then as

$$V_0 = \frac{A_0^2}{4\pi L_0} \tag{8}$$

The stretched sample at extension ε should have length L, radius r, and area A. The volume of the stretched sample is given in analogy to (8) by the relation

$$V = \frac{A^2}{4\pi L} \tag{9}$$

Assuming volume constancy during stretching, i.e. $V_0 = V$, a simple relation between length and surface area values results

$$\frac{A^2}{A_0^2} = \frac{L}{L_0} \tag{10}$$

Using the definition of the engineering strain Eq. (7), the relation between extension and the ratio of respective surface areas can be deduced

$$\frac{A}{A_0} = \sqrt{\varepsilon + 1}\,. \tag{11}$$

For the temperature increase ΔT of a sample in the magnetic field of constant high frequency with field strength H we found before Eq. (4). From (4) follows for a stretching experiment at constant field strength H, heat conductivity α, and constant magnetic field resistance constant R_H, a relation for the temperature steps with and without stretching and the respective surface areas

$$A_\varepsilon \Delta T_\varepsilon = A_{\varepsilon=0} \Delta T_{\varepsilon=0} \tag{12}$$

With (6) or (11) follows the final relation for a description of temperature vs. elongation experiments:

$$\frac{\Delta T_{\varepsilon}}{\Delta T_{\varepsilon=0}} = \frac{1}{\sqrt{\varepsilon+1}} = \frac{1}{\sqrt{\lambda}} \tag{13}$$

This equation states that the temperature increase ΔT of a sample at constant magnetic field strength H should be inversely proportional to the square root of the stretch ratio.

4. Model validation

4.1 Heat generation in an alternating magnetic field

First, the influence of MNP content on heating was investigated by exposing the SMPNCs to a high frequency magnetic field (258 kHz) at six different constant field strengths H in the range between 7 and 27 kA·m^{-1}. It can be seen (Fig. 2) that at constant H, the nanocomposites with higher MNP content reaches a higher T_{max}.

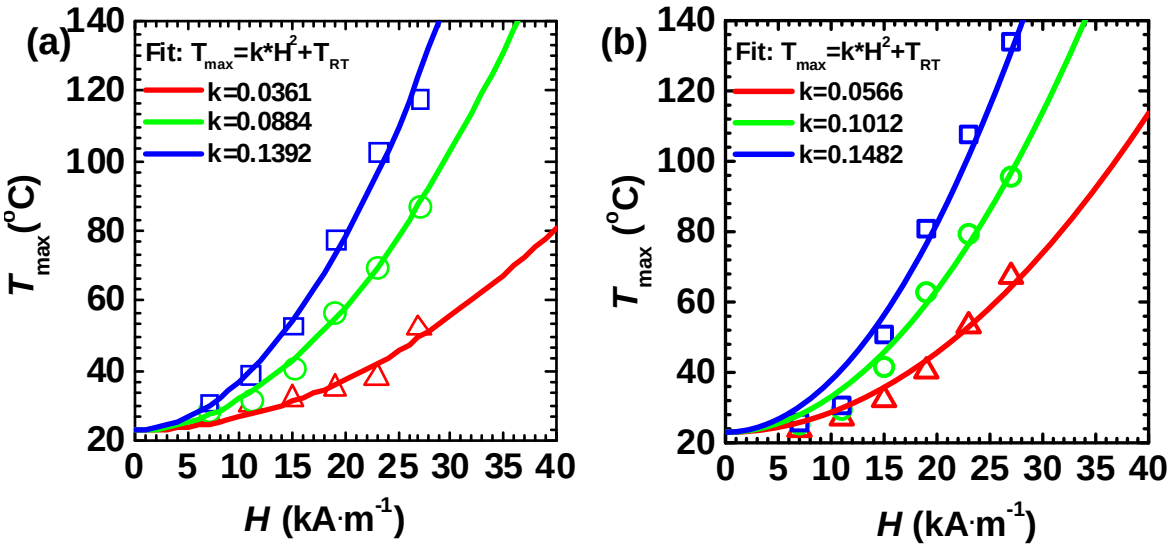

Fig. 2. Maximum achievable temperature T_{max} as function of applied H . Solid lines present fits of experimental data based on Eq. (3). (a) cPCLC systems: cPCLC05 (red triangle), cPCLC10 (green circle), cPCLC15 (blue square). (b) PEUC systems: PEUC05 (red triangle), PEUC10 (green circle), PEUC15 (blue square).

The respective fits of the experimental data points with model Eq. (4) are shown in Fig. 2 as well. The obtained k-values are presented in the upper left corner of the graphs. For room temperature T_{RT} a value of 23 °C was utilized. With increasing the amount of MNP in cPCLC and PEUC higher T_{max} were achieved at the same applied H, indicated also by higher k-

values. Similarly, increasing H led to higher equilibrium temperatures. T_{max}, in PEUC15, e.g., increased from about 53 °C to about 107 °C when H was raised from 15 to 23 kA·m^{-1}. Similarly T_{max} of cPCLC15 increased from 50 °C to 101 °C by changing H from 15 kA·m^{-1} to 23 kA·m^{-1}. Overall, the magnetic heating experiments of the SMPNCs at constant S/V ratio are well described by the model for the temperature increase, Eq. (4), with its quadratic proportionality to H.

4.2 Influence of surface area on T_{max}

The influence of the S/V ratio was further investigated with a set of experiments where samples of cPCLC10 with identical volume V but different surface areas A were prepared. The sample cPCLC10_A$_1$ had a surface area of A_1 = 825 mm^2, cPCLC10_A$_2$ of A_2 = 430 mm^2, and cPCLC10_A$_3$ of only A_3 = 240 mm^2. It should be noted that the sample cPCLC10_A$_2$ is identical with the sample named "cPCLC10" (see Fig. 2a and Table S1) which represents the "reference" for our set of samples with different S/V ratio. For all three samples the maximum temperature was measured as before in the high frequency magnetic field (258 kHz) at a constant H in the range between 7 and 27 kA·m^{-1}. The experimental T-values, already reported in [17], are presented in Fig. 3.

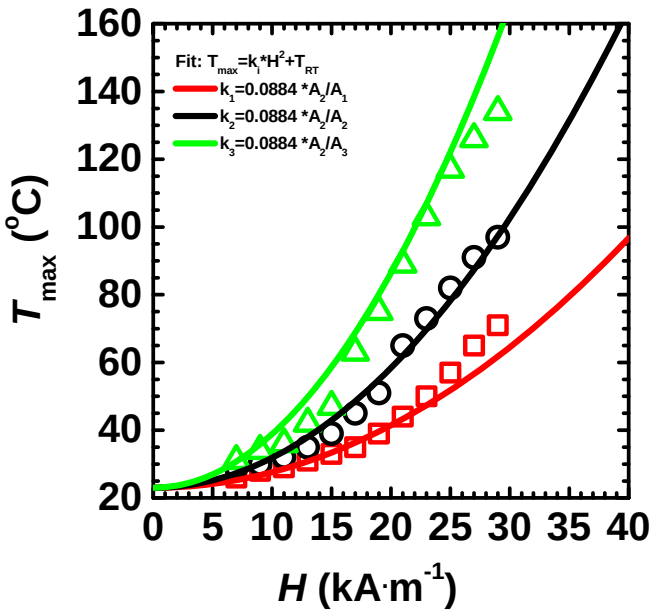

Fig. 3. Maximum achievable temperature T_{max} as function of applied magnetic field strength H for the sample cPCLC10 with different surface area at constant sample volume: $A_1 = 825$ mm^2 (red square), $A_2 = 430$ mm^2 (black circle), $A_3 = 240$ mm^2 (green triangle). Fits of experimental data (solid lines) are based on Eq. (4) with the respective k-values.

An increasing surface area, at constant sample volume, decreases the maximum temperature T_{max}, at a constant H. The inductively created heat per time unit can be released over a larger area, and therefore the temperature increase of the sample is lower. A very well fit of these data was possible (see curves in Fig. 3) with Eq. (4) and a surface area ratio (A_2 / A_i) ($i = 1,2,3$) with respect to the reference surface area of sample cPCLC10 (i.e. cPCLC10_A_2). Before, a k-value of 0.0884 was obtained for this sample (see Fig. 2a). Background of the inverse proportionality of factor $k \approx 1/A$ with the surface area is simply Fourier's law describing the emission of the inductive created heat. At constant heat flow rate $\dot{q}$, the temperature increase ΔT is given by Eq. (3). From Eq. (4) it can be read that the parameter k is inversely proportional to the surface area $k \approx 1/A$. We can also summarize the influence of the surface area A of a sample (of constant volume) on the obtained inductive temperature increase $\Delta T(A)$ of this sample at constant field strength H in the relation

$$\Delta T(A) = \frac{A_0}{A} \Delta T(A_0) \tag{14}$$

where $\Delta T(A_0)$ represents the inductive temperature increase if a sample of equal volume has a reference surface area A_0.

4.3 Changes in S/V ratio during uniaxial deformation

When a SMPNC sample is uniaxially elongated during magnetically heating at fixed H and f, the T_{max} of the test specimen should decrease, accordingly to model Eq. (13), depending on the change in the samples' geometry characterized by an increase in the surface area to volume ratio. The surface temperature of the sample results from the equilibrium between heat generation and heat loss by transfer to the environment during inductive heating. As the surface area A of the SMPNC increases during stretching, resulting in a new equilibrium, the value of T_{max} would decrease at each elongation step. The influence of deformation on T_{max}, was investigated by a simultaneous recording of the strain ε and the temperature T under magnetic field influence by using an IR pyrometer. The resulting data are shown in Fig. 4.

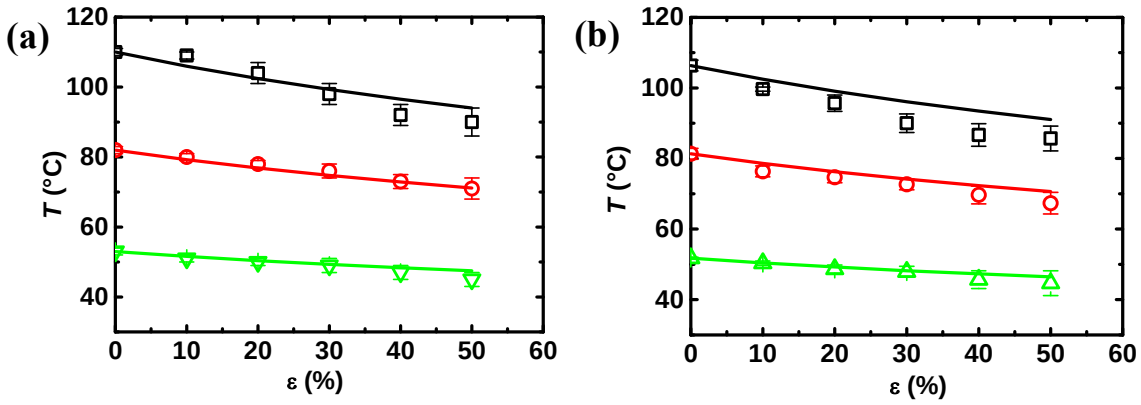

Fig. 4. Effect of stretching on the surface temperature of polymer composites at exposure to different values of magnetic field strength H. Curves present predictions with Eq. (4).
(a) cPCLC15: 23 kA·m^{-1} (black square), 19 kA·m^{-1} (red circle), 15 kA·m^{-1} (green triangle).
(b) PEUC15: 23 kA·m^{-1} (black square), 19 kA·m^{-1} (red circle), 15 kA·m^{-1} (green triangle).

By exposing the nanocomposite PEUC15 to a field strength of H = 23 kA·m^{-1}, an initial $T_{\max,\varepsilon=0}$ of around 107 °C was obtained within 2 minutes. After $T_{\max,\varepsilon=0}$ was achieved, a stepwise elongation of the sample (increment; $\Delta\varepsilon$ = 10%) and temperature measurement was carried out while H was kept constant (see Fig. 4b). At each deformation step the sample was allowed to reach equilibrium for five minutes, before the temperature was recorded with an IR pyrometer. After ε_m = 50%, a decrease of around 20 °C in the surface temperature $T_{\max}$ of the PEUC15 was achieved and a final $T_{\max,\varepsilon=0.5}$ of 86 °C was recorded. The higher the $T_{\max,\varepsilon=0}$, the higher was the decrease and the resulting temperature difference ($T_{\max,\varepsilon=0}$ - $T_{\max,\varepsilon}$). At H = 19 kA·m^{-1} a temperature drop of 14 °C and at H = 15 kA·m^{-1} of 7 °C was recorded.

The temperature decrease at the surface $T_{\max,\varepsilon=0}$ - $T_{\max,\varepsilon}$ during deformation in the magnetic field to an elongation ε can be described by the model relation, derived in the last section. Important is that during stretching the surface area of the sample A_ε increases ($A_\varepsilon > A_{\varepsilon=0}$), and the constant heat flow in a stretched sample will occur at a lower temperature difference $\Delta T_\varepsilon = T_{\max,\varepsilon} - T_{RT}$ between sample and surrounding. The ratio of stretched and unstretched ($\varepsilon = 0$) temperature differences is given by Eq. (13), where $\Delta T_{\varepsilon=0}$ is the temperature difference of the sample in the magnetic field to the environmental temperature. For, e.g., $T_{\max}$ = 81 °C and environmental temperature of 23 °C follows a temperature difference of $\Delta T_{\varepsilon=0}$ = 58 °C. If the sample is deformed to ε_m = 50%, i.e. ε = 0.5, a predicted temperature difference

of only $\Delta T_{\varepsilon=0.5} = 47$ °C follows from Eq. (13), which would be a decrease of 11 °C. This theoretical value was in acceptable agreement with the experimentally determined value of 14 °C. The curves in Fig. 4 were calculated by application of Eq. (13). For the lowest H the experimental data points are represented very well by the prediction of Eq. (13). For higher H, respectively temperatures, the deviations were found to increase, but the qualitative trend is well preserved. For the deformations up to 50%, the experimental $T_{\max,\varepsilon}$-values could be predicted by the model with an accuracy below 6%.

The just described effect of surface temperature decrease is not depending on the chemical nature of the matrix polymer as illustrated in Fig. 4a which represents also the same uniaxial stretching experiments for the polyurethane sample. The description of the data points for PEUC15 by the model Eq. (13) was similar to the cPCLC-system.

4.4 Application of the S/V ratios in a design example for a device

The just discussed S/V ratio may also be applied for selective shape changes of SMPNC samples in the magnetic field. It is possible to stepwise open a rolled strip of SMPNC. This may be the basis for a targeted design of a spiral-like device which can be opened to a certain point, controlled by magnetic field strength. A sketch is given in Fig. 5.

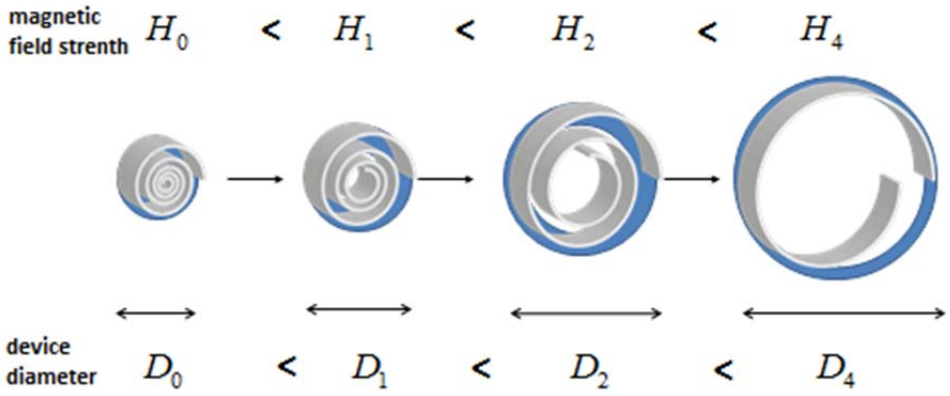

Fig. 5. Sketch of a spiral-like SMPNC device, presented by a ring. Depending on the S/V ratio, a certain magnetic field strength H is required to heat the device to $T \geq T_{sw}$ and to initiate the untwisting of the spiral. This recovery process of the shape-memory material results in an enlargement of the outer diameter D and is combined with an increase of the S/V ratio and decrease of T. At constant H, the process stops at $T < T_{sw}$. The untwisting of the spiral by stepwise increased H leads to the enlargement of D in stages.

Outside of the magnetic field $H_0 = 0$, the ring has the initial diameter D_0. By stepwise increasing the magnetic field strength *H*, the diameter of the ring can be increased to certain values. Results of shape-changing experiments are shown for a preliminary prototype out of cPCLC10 which was rolled at a temperature of 70 °C, and then cooled down again to room temperature (see Fig. 6, far left).

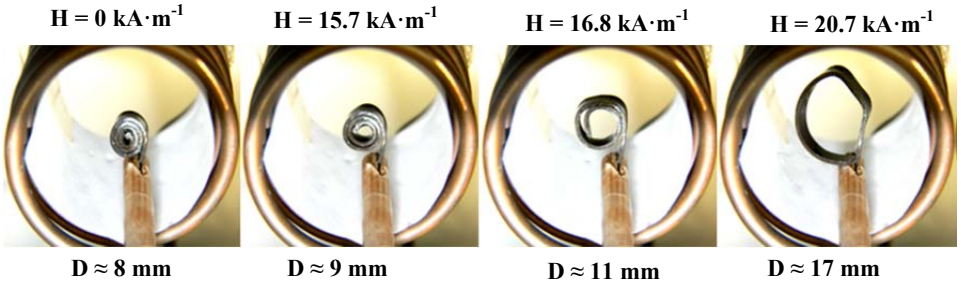

Fig. 6. Stepwise opening of a rolled compact strip of cPCLC10 by increasing field strength.

The sample in a compact rolled state had the lowest S/V ratio with an outer diameter of about $D \approx 8$ mm. It required a value of *H* of 15.7 kA·m^{-1} to heat the sample above T_{sw}. A stepwise uncoiling up to a diameter of about $D \approx 9$ mm took place till the sample temperature fell again below T_{sw}, and the uncoiling stopped. A further uncoil-step up to an outer diameter of about 11 mm could be created at a higher field strength of 16.8 kA·m^{-1}. Finally, the complete enrollment of the polymer stripe was achieved at the maximum value of $H = 20.7$ kA·m^{-1} ($D \approx 17$ mm).

An analysis of the shape transformation of the rolled stripe in the magnetic field as presented in Fig. 6 is possible on the basis of the obtained results for the surface to volume ratio. We consider the rolled stripe sample as a hollow cylinder of constant volume V_{HC}. This volume is equal to the volume of the extended stripe $V_S = l*h*t$ where *l*, *h*, and *t* represent length, height, and thickness of the stripe. Volume V_{HC} and surface area A_{HC} can be represented by the following equations

$$V_{HC} = \pi h(R^2 - r^2) \tag{15}$$

$$A_{HC} = 2\pi\left[(R+r)h + R^2 - r^2\right] \tag{16}$$

where R and r represent outer and inner radius of a hollow cylinder. At constant height h of the cylinder (equals to the height h of the strip), and assumption that the stripe volume V_S is equal to the volume of the hollow cylinder, $V_S = V_{HC}$, Eq. (15) allows the determination of the inner radius r for a given outer radius R.

$$r = \sqrt{R^2 - \frac{V_S}{\pi h}} \tag{17}$$

The surface area of the hollow cylinder given by Eq. (16) can be represented as function of only the outer radii $A_{HC}(R)$. Now, it is possible to predict T_{max}-values for the hollow cylinder of different outer radius R or outer diameters $D = 2R$. Necessary is only a k-value for the polymer nanocomposite at a certain surface area (A_0) in the relation Eq. (4). For the rolled strip these data are available, because the strip was formed out of cPCLC10, and the k-value for the reference sample (cPCLC10A2) was determined to $k = 0.0884$ with the surface area A_0 = 430 mm^2 (Fig. 3). For the rolled strip-sample the smallest outer diameter is $D_{min} = 8.0$ mm (nearly full cylinder) and the maximum diameter is $D_{max} = 16.8$ mm (circular ring). Fig. 7 presents the calculated T_{max}-values for the hollow cylinder for outer diameters $D_{min} \le D \le D_{max}$ for five different magnetic field strengths.

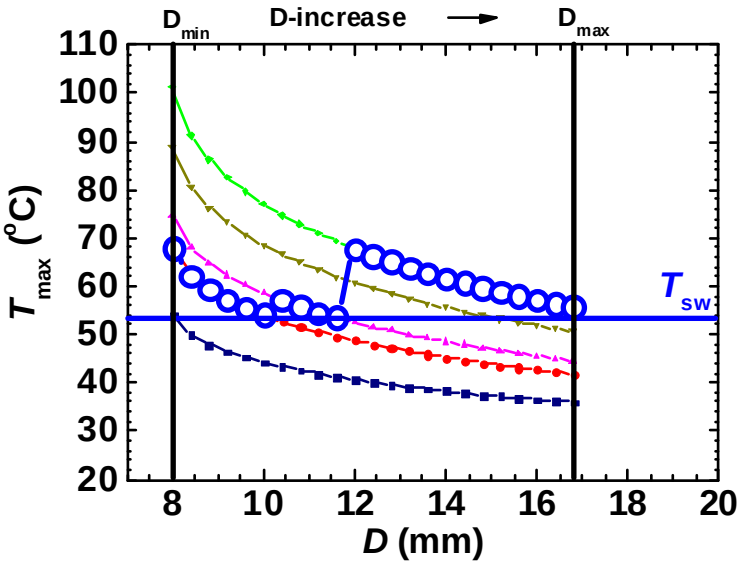

Fig. 7. Predicted temperature T_{max} vs. outer diameter (D) profiles for the stepwise opening of a rolled compact SMPNC strip of cPCLC10 by increasing field strength H. Lines with symbols present the functional relationship $T_{max}(D)$ in the diameter range $D_{min} \le D \le D_{max}$ for fixed H-values: 13 kA·m^{-1} (dark blue square), 15.7 kA·m^{-1} (red circle), 16.8 kA·m^{-1} (magenta triangle), 19.0 kA·m^{-1} (dark yellow triangle down), 20.7 kA·m^{-1} (green diamond). The connected blue open points represent qualitatively the path of the uncoiling experiment shown in Fig. 6, where stepwise opening was observed above the switching temperature T_{sw}.

Because the surface area A_{HC} increases for the constant volume hollow cylinder with increasing outer diameter, the T_{max} -value decreases. For the shape-recovery of the rolled sample it is important that the switching temperature T_{sw} (here approximately the T_m of the sample) is exceeded. This does not happened at a field strength of e.g. H = 13 kA·m^{-1}, but at a field strength of H = 15.7 kA·m^{-1}, the fully rolled stripe with $D \approx D_{min}$ would reach a temperature of about 68 °C, well above the T_{sw} of about 52 °C. A recovery process would start combined with an increase of the surface area but also linked with a temperature decrease. The recovery (uncoiling) will stop if the temperature of the sample reaches values below the transition temperature. The finally reached outer diameter D in this model calculation is about 10 mm. A further increase of the magnetic field strength to H = 16.8 kA·m^{-1} would increase T_{max} to about 60 °C. This temperature is again above the transition temperature and the recovery process would progress a step further. The predicted $T_{max}(D)$ curve with respect to the field strength values presented in Fig. 6, appears in Fig. 7 as the blue highlighted saw-tooth curve of connected open points.

Conclusion

A heat transfer model was proposed to predict the T_{max} values in SMPNCs achieved during inductive heating, when the samples are stretched to a certain deformation. Important is the change of surface area. It was found that the temperature increase ΔT for a sample at constant magnetic field strength H is inversely proportional to the square root of the extension ratio.

The model results were validated with magnetic heating experiments on two different polymer-MNP systems. Shape-memory composites cPCLC and PEUC with MNP contents between 5 to 15 wt% were remotely heated in an AMF of fixed frequency (f = 258 kHz). The heat transfer models allowed to predict the effect of applied H and the surface area of the SMPNCs on the T_{max} achieved during inductive heating. The surface temperatures of the SMPNCs were examined by exposing samples to different values of applied H between 7 and 27 kA·m^{-1} and were correlated with the theoretically predicted temperatures T_{max} using the heat transfer models. No appreciable differences in the heating capability of the SMPNCs, based on the morphological nature (crystalline and amorphous) of the polymer matrix, were observed. Finally, the model was applied as design tool for a ring-like device, where the diameter can be increased in a controlled way by the magnetic field strength. Experimentally, a controlled opening of a rolled compact SMPNC stripe of cPCLC10 was carried out by step wise increasing the value of H and measuring the increase in the outer diameter D of the stripe. The temperature as a function of outer diameter was successfully predicted at different

values of H and was compared with the experimental temperature profile. The temperatures predicted using the models were found to be in good agreement with the experimentally observed values. The established modeling approach will provide a better understanding of the heating of the shape-memory SMPNCs by various mechanisms and in a variety of heat transfer environments.

Finally, the demonstration experiment of an programmed rolled cPCLC stripe, where the uncoiling can be controlled by stepwise increasing the magnetic field strength H, is a clear indication that changes in S/V ratio of SMPNCs during the shape-recovery process can be applied in the future as control principle of SMPNCs, whereby the developed heat transfer model is capable to predict the resulting changes in T_{max}. With the model relation, a possible design criterion is developed to adapt the diameter of a spiral device to a certain size. This multi-shape effect by tailored geometry enables highly complex and controlled shape changes and could be applied in more complex shape-memory effects together with other stimuli, like IR or electric charge.

Acknowledgement

The authors would like to thank the Helmholtz-Association for funding.

References:

1. Behl M, Razzaq MY, and Lendlein A. Advanced Materials 2010;22(31):3388-3410.
2. Gunes IS and Jana SC. Journal of Nanoscience and Nanotechnology 2008;8(4):1616-1637.
3. Hsu L, Weder C, and Rowan SJ. Journal of Materials Chemistry 2011;21(9):2812-2822.
4. Leng J, Lan X, Liu Y, and Du S. Progress in Materials Science 2011;56(7):1077-1135.
5. Madbouly SA and Lendlein A. Advances in Polymer Science 2010;226:41-95.
6. Meng H and Li G. Polymer 2013;54(9):2199-2221.
7. Ratna D and Karger-Kocsis J. Journal of Materials Science 2008;43(1):254-269.
8. Xie T. Polymer 2011;52(22):4985-5000.
9. Buckley PR, McKinley GH, Wilson TS, Small W, Benett WJ, Bearinger JP, McElfresh MW, and Maitland DJ. Ieee Transactions on Biomedical Engineering 2006;53(10):2075-2083.
10. Golbang A and Kokabi M. Multi-Functional Materials and Structures Iii, Pts 1 and 2 2010;123-125:999-1002.
11. He Z, Satarkar N, Xie T, Cheng Y-T, and Hilt JZ. Advanced Materials 2011;33(28):3192-3196.
12. Koerner H, Price G, Pearce NA, Alexander M, and Vaia RA. Nat. Mater. 2004;3(2):115-120.

13. Narendra Kumar U, Kratz K, Heuchel M, Behl M, and Lendlein A. Advanced Materials 2011;23(36):4157-4162.
14. Narendra Kumar U, Kratz K, Wagermaier W, Behl M, and Lendlein A. Journal of Materials Chemistry 2010;20(17):3404-3415.
15. Mohr R, Kratz K, Weigel T, Lucka-Gabor M, Moneke M, and Lendlein A. Proceedings of the National Academy of Sciences of the United States of America 2006;103(10):3540-3545.
16. Razzaq MY, Behl M, Kratz K, and Lendlein A. Advanced Materials 2013;25(40):5730-5733.
17. Razzaq MY, Behl M, Kratz K, and Lendlein A. Advanced Materials 2013;25(38):5514-5518.
18. Razzaq MY, Behl M, and Lendlein A. Advanced Functional Materials 2012;22(1):184-191.
19. Vialle G, Di Prima M, Hocking E, Gall K, Garmestani H, Sanderson T, and Arzberger SC. Smart Materials & Structures 2009;18(11):115014.
20. Weigel T, Mohr R, and Lendlein A. Smart Materials & Structures 2009;18(2):025011.
21. Cui J, Kratz K, and Lendlein A. Smart Materials & Structures 2010;19(6):065019.
22. Solis-Correa RE, Vargas-Coronado R, Aguilar-Vega M, Cauich-Rodriguez JV, San Roman J, and Marcos A. Journal of Biomaterials Science-Polymer Edition 2007;18(5):561-578.
23. Lendlein A, Schmidt AM, Schroeter M, and Langer R. Journal of Polymer Science Part A-Polymer Chemistry 2005;43(7):1369-1381.
24. Cui J, Kratz K, Heuchel M, Hiebl B, and Lendlein A. Polymers for Advanced Technologies 2011;22(1):180-189.
25. Razzaq MY, Behl M, Kratz K, and Lendlein A. Materials Research Society Symposium Proceedings 2009;1140:185-190.
26. Pacull J, Gonçalves S, Delgado ÁV, Durán JDG, and Jiménez MaL. Journal of Colloid and Interface Science 2009;337(1):254-259.
27. Kroell M, Pridoehl M, Zimmermann G, Pop L, Odenbach S, and Hartwig A. Journal of Magnetism and Magnetic Materials 2005;289:21-24.
28. Rosensweig RE. Journal of Magnetism and Magnetic Materials 2002;252(1-3):370-374.
29. Incropera F and DeWitt D. Introduction to Heat Transfer: John Wiley and Sons, 1985.

Supplementary information

Table S1: Thermal properties of the polymer nanocomposites (SMPNCs)

Sample ID	μ_{mag} **(wt%)**[a]	$T_{\delta,max}$ **(°C)**[b]	T_m **(°C)**[c]	$T_{max,27}$ **(°C)**[d]
cPCLC00[0]	0.0	-42	52	-
cPCLC05[0]	4.4	-41	51	52
cPCLC10[0]	11.0	-40	52	87
cPCLC15[*]	15.4	-35	51	118
PEUC00[#]	0.0	74	-	-
PEUC05[#]	4.5	74	-	67
PEUC10[#]	11.0	74	-	96
PEUC15[#]	15.1	76	-	134

[a] The wt% of MNP determined by TGA
[b] Temperature at the peak maximum of the tan δ determined by DMTA
[c] Melting temperature determined by DSC
[d] Maximum achievable temperature at magnetic field strength $H = 27\ kA \cdot m^{-1}$.
[0] Data from Ref. [25]
[*] This work
[#] Data from Ref. [18]